Grain-boundary diffusion and segregation of gold in copper: Investigation in the type-B and type-C kinetic regimes

T. Surholt, Yu. M. Mishin,* and Chr. Herzig

Institut für Metallforschung, Universität Münster, Wilhelm-Klemm-Strasse 10, D-48149 Münster, Germany

Grain-boundary (GB) impurity diffusion of Au in Cu has been investigated by the radiotracer serial-sectioning technique using the ^{195}Au isotope with high specific activity. Measurements in the temperature ranges 618 to 1036 K and 450 to 526 K were carried out in Harrison's type-B and type-C regimes, respectively. In the type-B regime, the product $P = sD_{GB}\delta$ was determined (s being the segregation factor, D_{GB} the GB-diffusion coefficient, δ the GB width), while in the type-C regime D_{GB} values were measured directly. Combining the obtained P and D_{GB} values and assuming $\delta = 0.5$ nm, the Au GB-segregation factor was evaluated. From the temperature dependence of s, the segregation enthalpy $H_s = -9.7$ kJ mol^{-1} has been obtained. GB self-diffusion in Cu in the type-B regime has also been studied by the same experimental technique using the tracer ^{64}Cu. The obtained $D_{GB} = P/\delta$ values for self-diffusion are systematically larger than D_{GB} values for Au in Cu, whereas for lattice diffusion the opposite interrelation holds. This observation is discussed in terms of a trapping of Au atoms during impurity GB diffusion.

I. INTRODUCTION

In recent years problems associated with grain-boundary diffusion (GBD) and grain-boundary (GB) solute segregation in metals have attracted much attention, first of all in connection with the technical importance of these phenomena. For example, the lifetime of many structural materials and microelectronic elements at intermediate temperatures is controlled by the kinetics of diffusion penetration of detrimental impurities along GB's and formation of strong GB segregation. Some types of segregating impurities have a beneficial effect on bulk properties of materials, the best documented example being the boron-induced improvement of ductility of Ni_3Al.[1] At the same time, GBD measurements can be used as an effective and sensitive tool to study fundamental mechanisms of GB-solute interaction.[2-6]

In the most accurate GBD measurements a very thin layer of a radiotracer with a high specific activity is deposited at the specimen surface, and the specimen is then subjected to annealing at a desired temperature T for a time t, after which the depth distribution of the tracer is analyzed by the serial-sectioning technique. The amount of the tracer which is diffused into the specimen is usually so small that it cannot in practice disturb the GB chemistry and structure, so the tracer atoms actually play the role of an "atomic probe" which is rather sensitive to the structure, to characteristics of point defects, and to other properties of the GB's. The interpretation of the penetration profiles obtained is based on the Fisher model[7] and its analytical solutions.[2] The experiments are normally conducted in the so-called type-B kinetic regime,[8] in which the GBD is quasisteady and the tracer penetration profiles depend only on the product $P \equiv sD_{GB}\delta$, where s is the equilibrium segregation factor, D_{GB} the GBD coefficient, and δ the GB width. It is assumed that the

segregation of the diffusing atoms follows a Henry-type isotherm, which in turn implies that the GB's remain far from saturation with the diffuser and offer only one type of segregation position with a single segregation enthalpy $H_s < 0$, so that $s \propto \exp(-H_s/RT)$. Thus, in the B regime only on the triple product P can be measured, whereas the principal characteristics of GB diffusion and segregation (s, D_{GB}, and δ) are not determined separately. This uncertainty sets serious obstacles to the interpretation of the experimental results and can be overcome in two ways.

(1) The segregation factor of the impurity can be measured directly in independent experiments. For this purpose the metal is doped with the studied impurity and is carefully annealed to provide its equilibrium segregation. The specimen is then fractured inside an Auger electron spectroscopy (AES) apparatus and is analyzed for GB chemical composition in the regions of intergranular fracture. From the obtained surface excess of the impurity, Γ (mol/m^2), one can calculate the product $s\delta \simeq \Gamma/c_v$ (c_v being the impurity volume concentration in mol/m^3) and then combine it with P values to obtain $D_{GB} = P/s\delta$. Unfortunately, this approach can be successfully applied only to intrinsically brittle materials, like ceramics or some intermetallic compounds, which can be fractured intergranularly. For ductile materials, including pure metals, direct AES-type segregation measurements are in most cases impossible. Until now such combined diffusion-segregation studies have been carried out only for Sn, Sb, and Ni impurities in Fe.[9-11]

(2) An alternative approach, which is equally applicable to brittle and nonbrittle materials, consists in combining standard B-regime measurements with measurements under C-regime conditions,[8] when the tracer diffuses almost exclusively along the GB's without appreciable leakage to the volume. In the C regime, which is realized

at lower temperatures compared with the B regime, the condition

$$\alpha \equiv s\delta/2(D_v t)^{1/2} \gg 1 \qquad (1)$$

is fulfilled (D_v being the volume diffusion coefficient) and the diffusion profile depends only on the GBD coefficient D_{GB}. Therefore in this regime one can directly determine D_{GB}. Comparing the obtained D_{GB} value with the P value extrapolated to this temperature from B-regime measurements at higher temperatures, one can calculate the segregation factor $s = P/D_{GB}\delta$ (δ is assumed to be 0.5 nm).[7] A great problem associated with this approach is that the total activity of the tracer that penetrates into the specimen along the GB's in the C regime is very small, and consequently measurements of diffusion profiles in this regime are extremely difficult. In the last decade only one report on a C-regime measurement appeared in the literature to our knowledge (^{63}Ni GBD in fine-grained NiO at 773 K).[12] Recently, however, more systematic and reliable C-regime investigations have become possible due to the use of carrier-free radioisotope layers on the specimens and a well-type intrinsic Ge γ detector with a large efficiency and a low background.[13,14]

At the present, direct D_{GB} measurements in the C regime have been performed for self-diffusion in silver[13] and for Te impurity diffusion in silver.[14] In the first case, an experimental estimation of the GB width δ in silver has been made, with the result $\delta \simeq 0.5$ nm being in good agreement with Fisher's model.[7] In the second case, the D_{GB} values obtained for Te in Ag were directly compared with those for GB self-diffusion in Ag. Although Te is quite a fast diffuser in the lattice of silver,[15] the GBD of Te appears to be slower than GB self-diffusion in Ag. This observation can be explained by trapping of Te atoms during their diffusion to certain positions in the GB structure to form "embryos" of a two-dimensional (2D) phase. From the obtained temperature dependence of s, the enthalpy $H_s = -43.29$ kJ/mol and the entropy $S_s \simeq -3.08R$ of Te segregation in Ag have been obtained.

The large s values are well consistent with the extremely low solubility of Te in silver.[16]

The purpose of the present work is to investigate GB diffusion and segregation of Au in Cu in a wide temperature range in which both B and C regimes can be conveniently realized. Since Cu and Au possess rather similar physical properties, the segregation effects in this system must be relatively weak. According to Losch and Kirschner,[17] the surface of Cu-Au solid solutions shows predominantly Au segregation which increases with decreasing temperature and/or the volume content of Au. No data are available, however, for GB segregation of Au in Cu or in Cu-Au alloys. Taking into account the high plasticity of pure Cu and Au, the GBD measurements offer the only possibility at present to evaluate GB segregation in this system. Furthermore, no direct measurements of D_{GB} values have been made for impurities with low or moderate segregation intensities to our knowledge. Such data are obtained in this study. Referring to the fact that volume diffusion of Au in copper[18] is faster than self-diffusion in copper[19] and taking into account the previous results for Te in silver,[14] we found it necessary to compare the obtained D_{GB} values for Au in Cu with those for self-diffusion in Cu. Unfortunately, no direct measurements of GB self-diffusion in Cu are available in the literature. Therefore, to make this comparison possible, we have additionally studied GB self-diffusion in Cu using the same Cu material and the same experimental technique. Preliminary results of these measurements, which are, however, sufficient for the comparison, are also reported in this paper.

II. EXPERIMENTAL PROCEDURES

A. Specimen preparation

Copper with a nominal purity of 99.999% was used in this work as a starting material. The following impurity contents (in wt. ppm) were reported by the supplier (Demetron, Hanau, Germany):

Ag	Ca	Fe	Ni	Pb	S	Sb	Si	Sn	Zn
<0.5	1	2	<0.5	1	1.5	<1	<0.5	<0.5	<0.5

In the initial state the material was inconvenient for GBD experiments because of a too-large grain size and a distinct porosity. To obtain a more appropriate structure of the material, it was given the following treatment.

The initial ingot was remelted in an electron-beam furnace under vacuum ($\sim 10^{-4}$ Pa). A cylindrical bar with a diameter of 11 mm was machined from the ingot with a lathe and subjected to repeated rolling to a final diameter of 8 mm. To avoid contamination with impurities the ingot was carefully etched with nitric acid both before the remelting and after each run of the rolling. After rolling the bar was sealed into a quartz tube under purified argon ($\sim 10^2$ Pa) and annealed in two steps: first at 473 K for 6 h (stress relaxation) and then at 873 K for 48 h (recry-

stallization). The subsequent treatments were different for specimens intended for B- and C-regime measurements. For B-regime measurements, one part of the copper bar was cut with a corundum saw into cylindrical specimens with a thickness of 5 mm and their faces were polished on grinding paper. The specimens were reduced in thickness to about 3 mm by pressing on a deformation machine and then subjected to the two-step annealing procedure as described above. To prepare a material for C-regime measurements, the rest of the copper bar was cut into 6-mm-thick cylindrical specimens which, after grinding their faces, were deformed by multiple rolling in directions parallel to their faces. This was done in two steps with the above-described heat treatment applied

after each step. The final thickness of the specimens was about 2 mm. The resultant grain sizes amounted to 300–400 and 50–80 μm for the specimens intended for B- and C-regime experiments, respectively. No porosity could be revealed by optical microscopy. The structure with the smaller grain size remained stable during C-regime experiments at low temperatures and provided an essentially higher level of measured tracer activity compared with the coarse-grained structure.

One face of each specimen was polished mechanically by standard metallographical procedures and then electrolytically. All specimens were sealed into quartz tubes under purified argon atmosphere ($\sim 10^2$ Pa) and annealed in the conditions (temperature T, time t) of the intended diffusion anneals. This prediffusion heat treatment was necessary in order to guarantee equilibrium GB segregation of spurious impurities in the conditions of the subsequent diffusion experiments.

B. Diffusion measurements

The carrier-free radiotracer ^{195}Au (half-life 183 days) was used in this work in the form of a 4M HCl solution with the initial specific activity of about 0.63×10^8 Bq/μg. After a proper dilution, a drop of the radioactive solution was put onto the surface of each specimen and dried. The resultant surface activities were $(2–3) \times 10^4$ and $(0.8–1.0) \times 10^5$ Bq for the specimens intended for B-regime and C-regime measurements, respectively. The specimens were sealed into evacuated ($\sim 10^{-4}$ Pa) quartz tubes, which were filled with purified (99.999%) argon under $\sim 10^2$ Pa pressure, and were annealed at 14 temperatures in the range from 450 to 1036 K. The temperatures were measured and controlled with Ni-NiCr or Pt-PtRh thermocouples with an accuracy of about ± 1 K. After the diffusion anneals the specimens were reduced in diameter with a lathe in order to eliminate the effect of lateral-surface diffusion. The thicknesses of the removed layers were about three times the preestimated penetration depth of the tracer into the GB's.

The tracer penetration profiles were measured by the sectioning technique. Thin parallel layers with a thickness of a few μm were sequentially removed from the surface of the specimen with a microtome. The weight of each removed section was measured on a microbalance with ± 5 μg accuracy to determine the penetration depth y. To establish identical counting conditions for all sections, they were put into standard polypropylene tubes and dissolved in equal amounts (300 μl) of diluted HNO$_3$. In some cases several sections were put in one tube to increase the level of measured activities. The radioactivities were determined with a well-type intrinsic Ge γ detector connected with a 4096-channel analyzer. The intensity of the 65.12-keV decay energy peak was measured, for which the peak-to-background ratio was the largest compared with the three other peaks (66.83, 75.7, and 77.8 keV). The count rates obtained were corrected for the half-life of the tracer and the background of the detector, which was quite small in the chosen narrow window around the 65.12-keV peak. Applying also long counting times, this was the way to measure small activi-

ties, e.g., during profile measurements in the C regime. Knowing the activities of the sections and their weights, the relative specific activity $\bar{c}$ was determined as a function of the penetration depth y.

For self-diffusion measurements in Cu, the radiotracer ^{64}Cu (half-life 12.7 h) with initial specific activity 0.26×10^6 Bq/μg was produced from the nuclear reaction ^{63}Cu(n,γ)^{64}Cu by means of exposing copper with natural isotope composition to neutron radiation at a reactor (GKSS Forschungszentrum, Geesthacht, Germany). Immediately after the irradiation the radioactive Cu was delivered within a few hours to Münster. It was dissolved in dilute HNO$_3$, dropped onto the surface of the specimens, and dried. Taking into account the very short half-life of the tracer the initial surface activities had to be relatively high and ranged from 2×10^5 to 10^6 Bq depending on the intended annealing time. The thickness of the tracer layer at the surface was about 100 nm. The coarse-grained copper material prepared for B-regime measurements was used for the self-diffusion experiments. The procedures of diffusion annealing and sectioning were essentially the same as described previously. To compensate to a certain extent for the short half-life of ^{64}Cu the counting of the removed sections was started from the sections corresponding to the deepest penetrations (the smallest activities). The activities of the sections were determined by measuring the intensity of the β radiation ($E_{\text{max}} \sim 600$ keV) of ^{64}Cu with high efficiency in a liquid-scintillation counter combined with an automatic sample changer.

III. EXPERIMENTAL RESULTS AND INTERPRETATION

A. Measurements in the B regime

Figure 1 shows several typical penetration profiles for Au diffusion in Cu measured in this work. At a first step of data processing, all of the obtained profiles (Table I) were treated as measured in the B regime. Accordingly, they were plotted as $\ln\bar{c}$ against $y^{6/5}$ and their GBD-related tails were approximated by straight lines [Fig. 1(a)]. From the slopes $\partial\ln\bar{c}/\partial y^{6/5}$ the values of P were calculated from the Whipple-Suzuoka equation[2]

$$P = sD_{\text{GB}}\delta = 2q^p D_v^r t^{-u}\left[-\frac{\partial\ln\bar{c}}{\partial y^{6/5}}\right]^{-p}, \qquad (2)$$

where $p = 1.667$, $q = 0.775$, $r = 0.500$, and $u = 0.500$ in typical experimental conditions when the parameter $\beta = P/2D_v^{3/2}t^{1/2} \gg 10^4$, with slight changes for other ranges of β (see Table I in Ref. 14). In the B regime this parameter must be sufficiently large ($\beta > 10$). Calculations of P from Eq. (2) require the knowledge of the volume diffusion coefficients for Au in Cu. Most appropriate for this purpose are the results by Fujikawa et al.[18] obtained for ^{195}Au diffusion in Cu single crystals of the same purity in the temperature range 633–982 K. These D_v values follow an Arrhenius relation $D_v = D_v^0\exp(-H_v/RT)$ with the frequency factor and the activation enthalpy

$y^{6/5}$ [$10^{-5}m^{6/5}$]

$y^{6/5}$ [$10^{-5}m^{6/5}$]

y^2 [$10^{-8}m^2$]

y^2 [$10^{-9}m^2$]
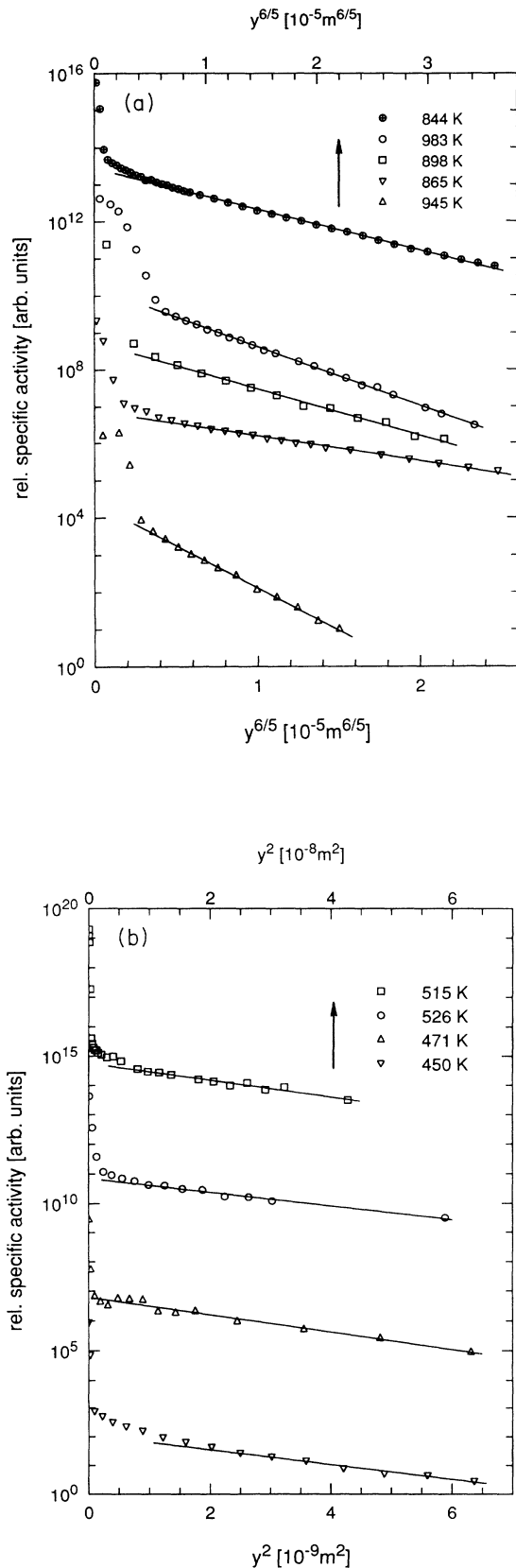
FIG. 1. Typical concentration-depth profiles for ^{195}Au diffusion in polycrystalline Cu in type-B (a) and type-C (b) kinetic regimes. Note that the profiles for 844 and 515 K refer to the upper scale.

$$D_v^0 = 0.803 \times 10^{-5} \, m^2 \, s^{-1} \, , \quad H_v = 191.046 \, kJ \, mol^{-1} \, ,$$

$$(3)$$

respectively. These data were used for the calculation of D_v in Eq. (2).

The P values obtained are listed in Table I and shown in Arrhenius coordinates in Fig. 2. The data points obey an Arrhenius dependence above ~ 600 K but considerably deviate from this dependence at lower temperatures. This type of behavior, which was earlier observed also for Te and self-diffusion in silver,[13,14] indicates that below ~ 600 K GBD is dominated by the transition regime between B and C and at lower temperatures by the C regime. Therefore, only the points in the temperature range 618–1036 K were interpreted as measured in the real B regime. With regard to α values, which must be small in the B regime, this suggestion will be verified later. All other conditions of this regime were fulfilled in this temperature range. Indeed, the maximal volume diffusion length $(D_v t)^{1/2}$ in this study was about 4 μm (at 983 K), i.e., much smaller than the grain size d, so the GB's were essentially isolated from each other. The requirement that β must be large was also met (see Table I). Since we tried to keep β values as high as possible, the annealing time was gradually reduced as the temperature increased (because $\beta \propto t^{-1/2}$). Nevertheless, at the highest temperature, 1036 K, β was already close to the limit of the B regime ($\beta \sim 10$). Since further essential decrease in t was not possible (because of uncertainties in t due to heating-up and cooling times), this temperature established the upper limit of possible B-regime measurements. Lastly, the initial thickness of the tracer layer at the specimen surface was smaller than $(D_v t)^{1/2}$, so Eq. (2) which implies Suzuoka's[20] instantaneous source conditions was applicable. The Arrhenius fitting to the B-regime points in the 618–1036-K range for ^{195}Au diffusion in Cu GB's yields

$$P \equiv s D_{GB} \delta$$

$$= (2.11^{+1.23}_{-0.78})$$

$$\times 10^{-15} \exp\left[-\frac{(81.24 \pm 3.08) \, kJ \, mol^{-1}}{RT} \right] \, m^3 \, s^{-1} \, .$$

$$(4)$$

The four penetration profiles measured so far for self-diffusion in Cu are shown in Fig. 3. Despite the short half-life of the ^{64}Cu tracer good GBD profiles could be measured, indicating that these experiments can be extended to lower temperatures in our forthcoming investigations. The parameter P for GBD was calculated from Eq. (2) using the volume self-diffusion coefficients D_v previously measured by Maier[19] on Cu single crystals of the same purity. In the high-temperature range these coefficients follow an Arrhenius relation with

$$D_v^0 = 1.0 \times 10^{-5} \, m^2 \, s^{-1} \, , \quad H_v = 196.8 \, kJ \, mol^{-1} \, . \quad (5)$$

The obtained values of P are given in Table II along with other related characteristics and are presented as an Ar-

TABLE I. Characteristics of grain-boundary diffusion of ^{195}Au in Cu determined from the experimental profiles assuming the type-B kinetic regime at all temperatures.

T (K)	t (s)	$(D_v t)^{1/2}$ (m)	$-\partial\ln\bar{c}/\partial y^{6/5}$ (m$^{-6/5}$)	P (m^3 s^{-1})	β	s	α
1036	4.25×10^3	2.82×10^{-6}	7.31×10^5	1.33×10^{-19}	12.6	2.7^a	2.4×10^{-4}
983	2.56×10^4	3.80×10^{-6}	3.66×10^5	9.63×10^{-20}	22.3	2.9^a	1.9×10^{-4}
945	1.04×10^4	1.52×10^{-6}	5.25×10^5	5.38×10^{-20}	80.1	3.0^a	4.9×10^{-4}
898	1.77×10^4	1.05×10^{-6}	2.94×10^5	5.80×10^{-20}	4.5×10^2	3.2^a	7.7×10^{-4}
865	2.49×10^5	2.41×10^{-6}	1.57×10^5	2.69×10^{-20}	2.4×10^2	3.4^a	8.5×10^{-3}
844	8.21×10^4	9.95×10^{-7}	1.79×10^5	2.74×10^{-20}	1.1×10^3	3.5^a	8.7×10^{-4}
786	2.62×10^5	6.51×10^{-7}	1.33×10^5	9.31×10^{-21}	4.4×10^3	3.9^a	1.4×10^{-3}
739	1.22×10^6	5.55×10^{-7}	9.52×10^4	2.99×10^{-21}	1.1×10^4	4.3^a	1.9×10^{-3}
666	5.34×10^5	6.67×10^{-8}	8.89×10^4	9.23×10^{-22}	8.3×10^5	5.1^a	1.8×10^{-2}
618	1.04×10^6	2.44×10^{-8}	6.96×10^4	2.61×10^{-22}	9.3×10^6	5.8^a	5.8×10^{-2}
526	1.02×10^5	2.96×10^{-10}	3.59×10^5	2.09×10^{-24}	4.1×10^9	7.9^b	6.6
515	1.11×10^6	6.12×10^{-10}	1.15×10^5	2.65×10^{-24}	6.4×10^9	8.4^b	3.5
471	1.11×10^6	7.62×10^{-11}	3.74×10^5	4.62×10^{-26}	5.8×10^{10}	11.3^b	37.4
450	2.85×10^6	3.91×10^{-11}	4.95×10^5	5.79×10^{-27}	1.4×10^{11}	11.1^b	70.2

^{a}Calculated from Eqs. (8) and (9).

^{b}Determined from comparison of D_{GB} values measured in the C regime with P values extrapolated from the B regime.

rhenius diagram in Fig. 2. An Arrhenius fit to these data gives

$$P \equiv D_{GB}\delta$$

$$= (1.16^{+0.53}_{-0.36})$$

$$\times 10^{-15}\exp\left[-\frac{(84.75\pm2.75)\text{ kJ mol}^{-1}}{RT}\right] \text{ m}^3\text{ s}^{-1},$$

(6)

for ^{64}Cu diffusion in Cu GB's. It is seen from Table II that the conditions of the B regime [$\alpha\ll1$, $\beta\gg1$, $(D_v t)^{1/2}\ll d$] were fulfilled.

B. Measurements in the C regime

The profiles measured at temperatures 450–526 K were treated as dominated by the C regime. Since the
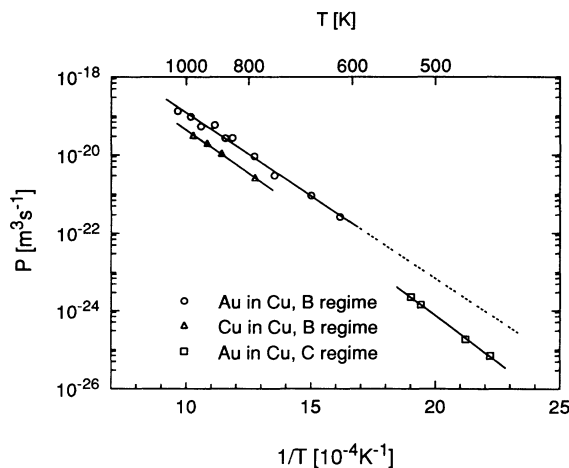
FIG. 2. Arrhenius diagram of ^{195}Au and ^{64}Cu diffusion along grain boundaries in Cu. For $T\leq526$ K, the grain-boundary diffusion coefficients D_{GB} for ^{195}Au in Cu were determined directly in the C regime; the obtained D_{GB} values are shown in this figure multiplied by $\delta=0.5$ nm. Note that the product $P=D_{GB}\delta$ obtained in this way does not take into account the Au GB segregation factor in Cu, s. The latter can be determined by combining these $D_{GB}\delta$ values with $P=sD_{GB}\delta$ values for ^{195}Au in Cu extrapolated from B-regime measurements made at higher temperatures (dashed line).

FIG. 3. Concentration-depth profiles for ^{64}Cu diffusion in polycrystalline Cu in the type-B kinetic regime.

TABLE II. Characteristics of grain-boundary self-diffusion in Cu determined from the experimental profiles in the type-B kinetic regime.

T (K)	t (s)	$(D_v t)^{1/2}$ (m)	$-\partial \ln\bar{c}/\partial y^{6/5}$ (m$^{-6/5}$)	P (m^3 s^{-1})	β	α^a
973	1.08×10^4	1.71×10^{-6}	7.57×10^5	3.10×10^{-20}	33.2	1.46×10^{-4}
923	1.07×10^4	8.82×10^{-7}	6.83×10^5	1.97×10^{-20}	1.5×10^2	2.83×10^{-4}
877	2.79×10^4	7.29×10^{-7}	4.93×10^5	1.08×10^{-20}	3.9×10^2	3.43×10^{-4}
784	4.38×10^4	1.84×10^{-7}	3.96×10^5	2.57×10^{-21}	9.0×10^3	1.36×10^{-4}

^{a}Calculated assuming $\delta = 0.5$ nm.

^{195}Au tracer source at the surface was very thin, the profiles were fitted by a Gaussian function, $\bar{c} \propto \exp(-y^2/4D_{GB}t)$. The GBD coefficients were therefore determined from the equation $D_{GB} = [4t(-\partial \ln\bar{c}/\partial y^2)]^{-1}$ using the slopes $\partial \ln\bar{c}/\partial y^2$ of the GB-related tails of the profiles [Fig. 1(b)]. Although the grain size was relatively small (50–80 μm) and carrier-free tracer material was used in this study, the measured activities were extremely low, so the GB-related tails of the profiles could be followed only in relatively narrow concentration ranges.

The results are listed in Table III and are shown on the Arrhenius diagram in Fig. 2. The values of $D_{GB}\delta$ obtained assuming the C regime at higher temperatures (> 618 K) strongly deviate from the Arrhenius dependence which otherwise nicely holds at $T \le 526$ K. This observation gives an additional confirmation that the high-temperature range was dominated by the B regime. An Arrhenius fit to the D_{GB} values for ^{195}Au diffusion along Cu GB's obtained at $T \le 526$ K gives

$$D_{GB} = (4.87^{+3.58}_{-2.06}) \times 10^{-6}$$

$$\times \exp\left[-\frac{(91.03 \pm 2.23) \text{ kJ mol}^{-1}}{RT}\right] \text{ m}^2 \text{s}^{-1} . \quad (7)$$

The condition $\alpha \gg 1$ which is associated with the C regime will be verified in the next section.

C. Determination of the segregation factor

The Arrhenius diagram in Fig. 2 demonstrates that the product $D_{GB}\delta(\delta = 0.5$ nm) is systematically smaller than the triple product $P = sD_{DG}\delta$ which additionally includes the segregation factor s. This observation indicates that (i) gold segregates to the GB's in copper ($s > 1$), and (ii) the degree of segregation increases with decreasing temperature. The segregation factor was calculated as

TABLE III. Characteristics of grain-boundary diffusion of ^{195}Au in Cu in the type-C kinetic regime.

T (K)	t (s)	$(D_v t)^{1/2}$ (m)	$-\partial \ln\bar{c}/\partial y^2$ (10^8 m^{-2})	D_{GB} (m^2 s^{-1})
526	1.02×10^5	2.96×10^{-10}	5.366	4.56×10^{-15}
515	1.11×10^6	6.12×10^{-10}	7.866	2.86×10^{-15}
471	1.11×10^6	7.62×10^{-11}	6.205	3.63×10^{-16}
450	2.85×10^6	3.91×10^{-11}	6.279	1.40×10^{-16}

$s = P/D_{GB}\delta$ using D_{GB} values directly determined in the C regime (Table III) and P values extrapolated from B-regime measurements according to Eq. (4). The results are listed in Table I. As was expected, the s values are relatively small and vary from 11 at 450 K to 6 at 526 K with an extrapolated value of ~ 2 at the melting point of copper. Since the amount of the tracer which was introduced into the GB's was extremely small, the segregation is assumed to follow a Henry-type isotherm. Then, the temperature dependence of s has the form

$$s = s_0 \exp(-H_s/RT) . \quad (8)$$

Fitting Eq. (8) to the experimental data (Fig. 4) yields

$$s_0 = 0.878^{+0.634}_{-0.368} , \quad H_s = -(9.69 \pm 2.20) \text{ kJ mol}^{-1} . \quad (9)$$

The entropy of GB segregation estimated from the preexponential factor s_0 equals $S_s \simeq (-0.13 \pm 0.54)R$. Strictly speaking, this means that S_s is zero within the experimental error.

Using the obtained values of s, we can now estimate the parameter $\alpha = s\delta/2(D_v t)^{1/2}$ in the low-temperature range (≤ 526 K). As is seen from Table I, α in this range is rather large (6.6–70.2) and well consistent with the C regime. Furthermore, α values can now be calculated also in the high-temperature range (≥ 618 K) using the segregation factors extrapolated from Eqs. (8) and (9). The resultant α values (Table I) are rather small (2.4×10^{-4}–5.8×10^{-2}) and consistent with the B regime
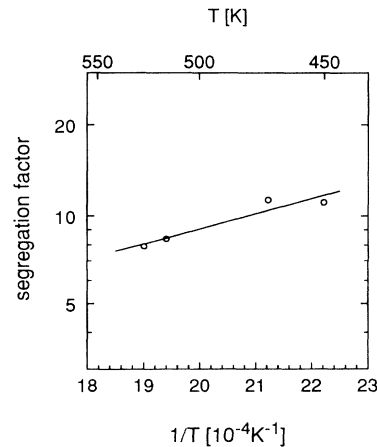
FIG. 4. Temperature dependence of Au grain-boundary segregation factor in Cu, obtained from grain-boundary diffusion data.

at these temperatures. This good agreement indicates that the assumed identification of the boundary diffusion regimes was correct.

IV. DISCUSSION

A. Grain-boundary diffusion in the B regime

The high-temperature (≥ 618 K) profiles for Au diffusion in Cu measured in this work followed the $\ln \bar{c} \propto y^{6/5}$ law [Fig. 1(a)] and were thus undoubtedly dominated by the B regime. Figure 5 and Table IV compare the obtained GBD characteristics with the literature data. The measurements by Austin and co-workers[21,22] were made on a bicrystal with a 45° [001] tilt GB in a relatively limited (898–1033 K) temperature range using electron-probe microanalysis. Au isoconcentration contours and GB concentration profiles were used to deduce the GB diffusivity. The results are rather close to our data, especially at high temperatures. In contrast, the P values obtained by Chatterjee and Fabian[23] on polycrystalline Cu using the serial-sectioning technique seem to be much too underestimated and lead to an unrealistically low activation enthalpy of $Q_{GB} \simeq 45$ kJ mol^{-1}. These data are regarded as unreliable.[24] Finally, Aleshin and co-workers[25,26] have recently studied volume and GB interdiffusion in Au-Cu thin films by the Rutherford backscattering technique. Comparison of their results with our data is not straightforward, first of all because the structural state of thin films is different from that of well-annealed massive specimens. Notably, the volume interdiffusion coefficients measured by Aleshin and co-workers[25,26] are much greater than the coefficients of tracer diffusion in massive single crystals, both for Au in Cu,[18] and for Cu in Au.[27] Also, the obtained activation enthalpy of volume diffusion, ~ 106 kJ mol^{-1}, is comparable with the one for GBD (~ 91 kJ mol^{-1}). These unusual features are explained[25,26] by the presence of structural defects in the volume of thin films. The enhanced volume diffusivity is evidently the reason why the GBD in Au-Cu thin films occurred in the B regime, while in our study the same temperature range was dominated by the C regime. It should also be mentioned that Au concentration in the GB-related parts of the profiles measured on Cu-Au thin films varied from a few at. % to 10–20 at. %, so these profiles represented GB interdiffusion rather than tracer impurity diffusion. It is
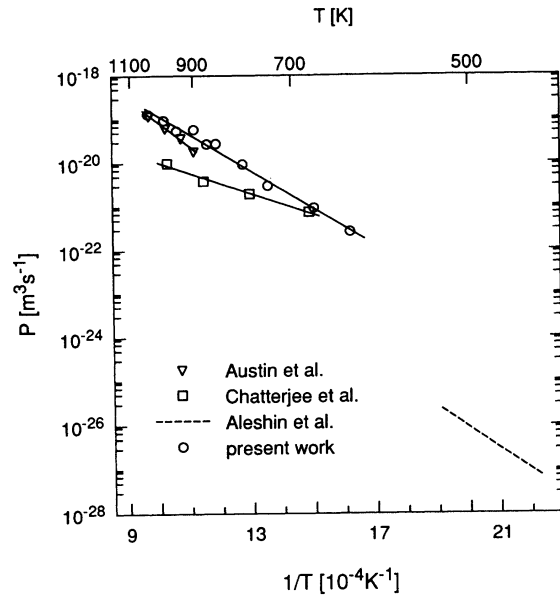
FIG. 5. Comparison of the GB diffusivity P of Au in Cu measured in this work with the literature data obtained by Austin and co-workers (Refs. 21,22), Chatterjee and Fabian (Ref. 23), and Aleshin and co-workers (Refs. 25,26).

not surprising, therefore, that, although Q_{GB} is in both cases comparable, the P values obtained by Aleshin and co-workers[25,26] and our P values extrapolated to the same temperature interval differ by nearly three orders of magnitude. As is seen from Fig. 5, our measurements extend to a wider temperature range. Also, due to the use of ^{195}Au radiotracer with high specific activity, the concentration of Au atoms was extremely small, so the results of the present work represent the real tracer impurity diffusion at infinite dilution.

Concerning GB self-diffusion in copper, the data available in the literature come from initial-stage sintering investigations,[28] creep experiments,[29] and theoretical calculations.[30] According to these indirect estimations, the activation enthalpy H_{GB} varies from 102 to 120 kJ mol^{-1}. Direct measurements performed in this work yield an appreciably smaller value of $H_{GB} \simeq 85$ kJ mol^{-1} [Eq. (6)]. The ratio $H_{GB}/H_v \simeq 0.43$ is well consistent with the vacancy mechanism of GBD.

TABLE IV. Comparison of the obtained Arrhenius characteristics of grain-boundary diffusion of Au in Cu with data from the literature. EPMA: electron-probe microanalysis; S: sectioning technique; RBS: Rutherford backscattering.

P_0 (m^3 s^{-1})	Q_{GB} (kJ mol^{-1})	Experimental method	Temperature range (K)	Reference
2.60×10^{-14}	105.01	EPMA	898–1033	Refs. 21,22
2.40×10^{-18}	45.46	S	673–973	Ref. 23[a]
2.50×10^{-17}	90.70	RBS	448–523	Refs. 25,26
2.11×10^{-15}	81.24	S	618–1036	present work

[a]Recalculated from the original data using the volume diffusion coefficients measured by Fujikawa et al. (Ref. 18).

B. Grain-boundary diffusion in the C regime

As was noted above, the high-temperature (≥ 618 K) profiles for Au GBD in Cu followed the relation $\ln\bar{c} \propto y^{6/5}$ which is characteristic of the B regime. In contrast, the C regime could not be unambiguously recognized from the shape of the low-temperature profiles (≤ 526 K). Because of the very low level of the measured radioactivities, the GBD-related tails of these profiles extended to relatively narrow (about one order of magnitude) concentration ranges and could be fitted both by a Gaussian function [cf. Fig. 1(b)] and by the $\ln\bar{c} \propto y^{6/5}$ law with nearly the same accuracy. Nevertheless, the C regime in this temperature range could be correctly identified from the behavior of the diffusion characteristics at different temperatures.

Indeed, according to the theoretical analyses by Atkinson and Taylor[12] and Szabo, Beke, and Kedves,[31] an inadequate processing of C-regime profiles according to the B regime results in apparent P values which are essentially underestimated compared with the true ones. Likewise, apparent D_{GB} values obtained by processing B-regime profiles according to the C regime essentially underestimate the true D_{GB} values. Therefore, all the experimental profiles for Au in Cu were at first tentatively processed according to both the B and C regimes. The P values obtained follow an Arrhenius relation, Eq. (4), at $T \geq 618$ K but lie significantly below the Arrhenius line at lower temperatures. Similarly, the diffusion coefficients D_{GB} obey an Arrhenius relation, Eq. (7), at $T \leq 526$ K but strongly deviate from it towards smaller values at higher temperatures. This behavior is perfectly consistent with the theoretical predictions and provides strong evidence that the temperature ranges $T \geq 618$ K and $T \leq 526$ K were dominated by the B and C regimes, respectively. An independent confirmation of this conclusion comes from the estimation of the parameter α using the obtained values of the segregation factor s: α has proven to be rather small at $T \geq 618$ K and rather large at $T \leq 526$ K in agreement with the definition of the regimes.

These results demonstrate once again that one cannot completely rely on the shape of GBD profiles measured on polycrystals, especially at low temperatures, in order to identify the C regime. The profile shape is affected by a number of factors which are not taken into account in the standard Fisher's model, such as (i) the presence of a spectrum of different types of GB's with diverse diffusion and segregation characteristics; (ii) different inclinations of GB's towards the specimen surface; (iii) direct tracer diffusion along single dislocations or/and subgrain boundaries near the surface, etc. Additionally, because of the low activity level the C-regime profiles are usually measured in limited concentration intervals and suffer from a considerable scatter of the data points. In such conditions the C regime should be identified not from the shape of each particular profile, but rather based on the analysis of general trends over the whole set of the experimental data, the way it was done in this study and in our previous works.[13,14] Weighty arguments in favor of this approach were obtained in our recent investigation of GB

self-diffusion in silver.[13] Some of the C-regime profiles in this work were measured in rather wide concentration ranges using carrier-free [105]Ag surface layers with very high activity obtained by implantation at the ISOLDE/CERN facility. These profiles had a clearcut downward curvature in the coordinates $\ln\bar{c}$ against $y^{6/5}$ and were well consistent with the Gaussian function, $\ln\bar{c} \propto y^2$. Since also α was large, the C regime was undisputed. Some other profiles, however, were measured in similar conditions (T,t) but using the tracer [110m]Ag with a lower specific activity, and their shape was equally consistent both with a Gaussian function and with the $\ln\bar{c} \propto y^{6/5}$ relation. Nevertheless, the GBD coefficients obtained from these two kinds of profiles were in good agreement with each other.

It should be emphasized that the possibility of C-regime measurements is a fundamental problem in GBD. Therefore we have to make some comments on the recent review by Klotsman[32] devoted in large part to this problem. According to Klotsman,[32] the real C regime has so far never been realized, and, moreover, cannot be realized in real materials. His arguments are based on the assumption that the tracer leakage from the GB's occurs to a so-called "pumping" zone which is supposed to exist around GB's at low temperatures. In this zone the tracer diffusion coefficient D_p is much larger than in the undisturbed lattice far from the boundaries. The formation of the pumping zone is explained by GB segregation of "residual interstitial impurities" which form highly mobile vacancy-impurity complexes and thereby significantly enhance the tracer diffusion. At high temperatures the tracer leakage is governed by the normal volume diffusivity D_v, but at low temperatures the segregation effects come into play and the tracer diffusion proceeds with a much higher rate, $D_p \gg D_v$. As a result, α decreases and the boundary diffusion remains always in the B regime whereas the C regime is never achieved. The downward curvature of the Arrhenius plot $\ln P$ against $1/T$ is then explained by using in Eq. (2) incorrect, underestimated D_v values at low temperatures. Substituting into this equation the "true" diffusion coefficient D_p would restore the normal Arrhenius dependence. It should be mentioned that a similar reasoning was earlier put forward by Kaygorodov et al.,[33] although the enhancement of tracer mobility around GB's was attributed by them to dislocation pipe diffusion.

In our view the arguments against the existence of the C regime are inconsistent with the available experimental data for the following reasons.

(i) As was mentioned above, the tails of the low-temperature (large-α) profiles for [105]Ag diffusion in silver[13] had a Gaussian shape and were obviously inconsistent with the B regime. Notably, Klotsman[32] has processed our C-regime profiles[13] according to the B regime paying no attention to their obvious downward curvature in the coordinates $\ln\bar{c}$ versus $y^{6/5}$. The obtained nonmonotonic, V-shaped dependence of $\ln(-\partial\ln\bar{c}/\partial y^{6/5})^{5/3}t^{1/2}$ on $1/T$ was interpreted by him as an argument in favor of the pumping mechanism. It can be easily understood, however, that this V-type behavior is nothing but a different representation of the downward

curvature of the Arrhenius plot $\ln P$ versus $1/T$, which can be explained by a change in GBD regime.

(ii) The directly determined D_{GB} and s values demonstrate a good Arrhenius-type behavior in relatively extended (~ 100 K) temperature intervals and yield very reasonable values both for δ (Ref. 13) and for the tracer segregation characteristics (see discussion below). The parameter α calculated using the obtained δ and s values and the normal volume diffusivity D_v is always well consistent with the assumed GBD regimes.

(iii) The transition temperature below which the effect of the pumping zone comes into play must sensitively depend on such factors as the dislocation density, the impurity content (especially with respect to fast-diffusing impurities), the regime of prediffusion heat treatment, etc. However, in all known cases the temperature at which the deviation from the Arrhenius behavior of P appeared was well reproducible and perfectly correlated with the temperature at which the condition $\alpha \sim 1$ (with the normal D_v) was achieved. This observation indicates that this transition was caused by a change in the GBD regime rather than by dislocation or impurity effects.

(iv) For GBD of Te in silver,[14] the apparent P value at the lowest temperature (378 K) was smaller than the value extrapolated from the high temperatures, at which the B regime was operative, by a factor of 10^6. To account for this large underestimation of P, D_p must be greater than D_v by a factor of 10^{12}. In other cases as well, the ratios D_p/D_v at low temperatures are also quite spectacular; for Au in Cu at 450 K $D_p/D_v \sim 10^4$. It is difficult to imagine a mechanism by which residual impurities can provide such a great enhancement in lattice diffusion of the tracer in fcc metals (especially for Te which is already a fast diffuser in silver[15]).

(v) In cases of fast-diffusing tracer impurities, like Te in silver,[14] the C regime may be established in spite of $(D_v t)^{1/2} \gg \delta$ due to large s, so that $\alpha \gg 1$ results, cf. Eq. (1). Then, the volume diffusion of the tracer is independent of the pumping zone which, according to Klotsman,[32] is confined to a narrow ($\sim \delta$) region around the GB's.

Thus, the arguments put forward by Kaygorodov et al.[33] and Klotsman[32] are untenable regarding the possibility of direct GBD measurements in the C regime established in this study and in our previous works.[13,14]

Gold impurity atoms diffuse faster and exhibit a smaller activation enthalpy compared with copper self-diffusion in the lattice [cf. Eqs. (3) and (5)]. This feature can be explained by elastic Au-vacancy interaction in the copper matrix (Au has a larger atomic radius than Cu). From this one could expect that Au GBD is also faster than Cu GB self-diffusion. In Fig. 6 we compare the directly measured GBD coefficient D_{GB} for Au in Cu with D_{GB} for GB self-diffusion in Cu calculated from Eq. (6) as P/δ with $\delta = 0.5$ nm. In contrast to volume diffusion, Au atoms diffuse along GB's in Cu more slowly and with a larger activation enthalpy ($H_{GB} \simeq 91$ kJ mol^{-1}) compared with Cu GB self-diffusion ($H_{GB} \simeq 85$ kJ mol^{-1}). A similar feature was previously observed for tellurium diffusion in silver,[14] although the effects were much stronger. In both cases, the observed behavior of
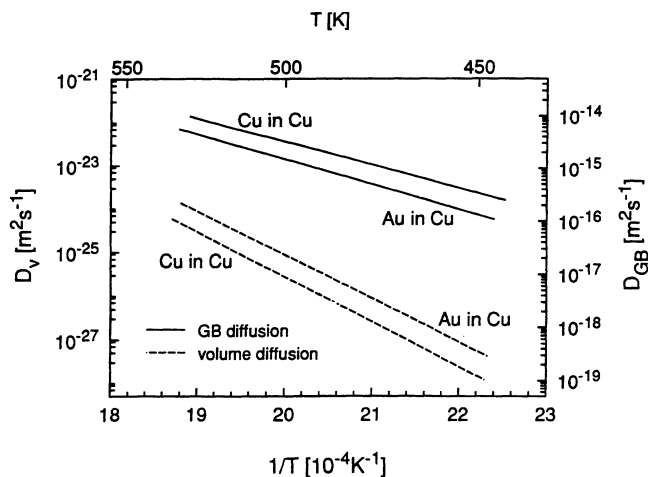
FIG. 6. Arrhenius diagram of the GBD coefficients D_{GB} for Au in Cu measured in the C regime and for self-diffusion in Cu calculated using the high-temperature $P = D_{GB}\delta$ values and assuming $\delta = 0.5$ nm. The corresponding volume diffusion coefficients D_v calculated using Eqs. (3) and (5) are shown for comparison.

GBD characteristics can be interpreted in terms of competition between (i) enhancement of impurity diffusion due to impurity-vacancy interaction, and (ii) trapping the impurity atoms to selected positions in the GB structure, where they become immobile and do not contribute to the net GB flux.

In the systems discussed, the second tendency evidently prevails over the first one. In the case of Te in Ag, it was suggested[14] that the trapping was caused by a tendency to form local ordered compounds which are probably similar to those that are present on the Ag-Te phase diagram. This explanation can be extended to the Cu-Au system where the components also form ordered intermetallic compounds (Cu_3Au, $CuAu$, and $CuAu_3$) below ~ 700 K. Since the GB structure offers a larger variety of atomic configurations than the lattice, the diffusing Au atoms can more readily find energetically favorable positions in which the local surroundings are similar to those in an ordered compound. Such immobile impurity-solvent complexes can be considered as "embryos" of a 2D phase.[3] Because each tracer atom has a chance to be captured by a trap, the GBD coefficient decreases and the effective activation enthalpy increases at the expense of the activation energy required to escape from the trap. The relatively small value of the segregation entropy, $S_s = (-0.13 \pm 0.54)R$, confirms the weak character of the trapping of Au atoms in Cu GB's. For Te in silver[14] S_s was significantly larger ($\sim -3R$), which was consistent with the existence of several compounds with high ordering energy on the Ag-Te phase diagram.[16]

C. Grain-boundary segregation of Au in Cu

Taking into account relation (8), the temperature dependence of the GB diffusivity P has the form

$$P = s_0 D_{GB}^0 \delta \exp(-Q_{GB}/kT) , \tag{10}$$

where the apparent activation enthalpy $Q_{GB} = H_{GB} + H_s$ includes both the true activation enthalpy of GBD, H_{GB}, and the (negative) segregation enthalpy H_s. In usual B-regime experiments only the apparent value Q_{GB} can be measured. In the present work by means of combined B- and C-regime measurements we have separately determined both the GBD characteristics, $D_{GB}^0 = 4.87 \times 10^{-6}$ $m^2 s^{-1}$ and $H_{GB} = 91.03$ kJ mol^{-1}, and the segregation characteristics s_0 and H_s [Eq. (9)] for Au in Cu. To our knowledge, no experimental investigations or computer simulations have ever been performed for Au-impurity GB segregation in Cu. Therefore the obtained GB-segregation characteristics can be compared only with the results for surface segregation and with rough theoretical estimations.

McDavid and Fain[34] studied the surface composition of Cu-Au thin films having (111) orientation by means of AES. The first layer was found to be significantly enriched in Au over the entire range of compositions studied. Later Losch and Kirschner[17] investigated, also by AES, the surface composition of polycrystalline Cu-(7.5–56.3 at. %) Au alloys in the temperature range from 473 to 823 K. Again it was found that the surface was enriched with Au and that the segregation factor decreased with increasing temperature and Au content in the volume. For the Cu-(7.5 at. %)Au alloy the segregation enthalpy $H_s \simeq -13.0$ kJ mol^{-1} was estimated. Even though this value appears to be of the same magnitude as our value $H_s \simeq -9.7 \pm 2.2$ kJ mol^{-1} relating to GB segregation, an extended discussion is required for full appreciation.

For theoretical estimations, H_s can be represented as a sum of a chemical term H_s^{ch} and an elastic term H_s^{el}: $H_s = H_s^{ch} + H_s^{el}$. The chemical contribution can be evaluated in terms of the "broken-bond" model which relates the segregation enthalpy to the change in the energy of broken chemical bonds at the GB due to segregation. Neglecting the regular solution parameter, for a binary solid solution A-B one has[35]

$$-H_s^{ch} = \tfrac{1}{2}(Z_v - Z_{GB})(\epsilon_{BB} - \epsilon_{AA}) , \qquad (11)$$

where Z_v and Z_{GB} are the coordination numbers of atoms across an interatomic plane in the volume and across the GB, respectively. In turn, the bond energies ϵ_{AA} and ϵ_{BB} can be related to the sublimation enthalpies of the pure components,

$$H_A^{sub} = -\tfrac{1}{2}Z\epsilon_{AA} , \quad H_B^{sub} = -\tfrac{1}{2}Z\epsilon_{BB} , \qquad (12)$$

Z being the coordination number in the lattice. Combining Eqs. (11) and (12),

$$-H_s^{ch} = \frac{Z_v - Z_{GB}}{Z_v} \times \frac{Z_v}{Z}(H_A^{sub} - H_B^{sub}) . \qquad (13)$$

Assuming, following Seah,[35] that $(Z_v - Z_{GB})/Z_v \simeq \tfrac{1}{6}$ and $Z_v/Z \simeq \tfrac{1}{4}$, Eq. (13) for the Cu-Au system finally becomes

$$-H_s^{ch} = \tfrac{1}{24}(H_{Cu}^{sub} - H_{Au}^{sub}) . \qquad (14)$$

Using the values $H_{Cu}^{sub} = 317$ kJ mol^{-1} and $H_{Au}^{sub} = 345$

kJ mol^{-1} estimated from the ln$p$ dependence on $1/T$ (p = the vapor pressure),[36] $H_s^{ch} \sim +1$ kJ mol^{-1} results from Eq. (14). The positive sign of H_s^{ch} implies that Cu must segregate to the GB's rather than Au, which obviously contradicts the experimental data. This inconsistency as well as the relatively small absolute value of H_s^{ch} indicate that for Au in Cu the chemical contribution to H_s is negligible.

The elastic term is associated with a strain release due to segregation of impurity atoms having a larger atomic size a_B than the solvent atoms (a_A). For surface segregation, Seah[35] proposed the semiempirical relation

$$-H_s^{el} \text{ (kJ mol}^{-1}) \simeq 4.64 \times 10^{31} a_A (a_B - a_A)^2 . \qquad (15)$$

Using the values $a_{Cu} = 2.28 \times 10^{-10}$ m and $a_{Au} = 2.57 \times 10^{-10}$ m calculated from the equation $a^3 = A/\rho$ (A = atomic mass, ρ = density), Eq. (15) yields $H_s^{el} \simeq -8.9$ kJ mol^{-1}. In spite of the rather approximate character of this estimation, the obtained value is well consistent with the experimental result[17] $H_s = -13.0$ kJ mol^{-1}. This agreement provides evidence that surface and probably also GB segregation in the system Cu-Au are dominated by the strain-release effect. Even though for GB segregation H_s^{el} must be somewhat smaller than follows from Eq. (15), it appears that the obtained value of H_s^{el} stands in reasonable agreement with our result $H_s \simeq -9.7 \pm 2.2$ kJ mol^{-1}.

Concerning our estimation of the segregation entropy for Au in Cu, $S_s \simeq (-0.13 \pm 0.54)R$, we point out that values of S_s ranging from 0 to a few R are known in the literature.[37] Our result is comparable, for example, with $S_s = (0 \pm 0.5)R$ obtained for indium segregation in symmetric $\langle 110 \rangle$ tilt GB's in nickel.[38] However, since the accuracy of the estimation of S_s is relatively low, we shall not discuss this result in more detail.

V. CONCLUSIONS

(1) GB impurity diffusion of ^{195}Au in Cu has been studied by the radiotracer sectioning technique in the temperature range 450–1036 K. Both type-B and type-C kinetic regimes were realized at temperatures $T \geq 618$ K and $T \leq 526$ K, respectively.

(2) The values of $P = sD_{GB}\delta$ measured in the B regime follow an Arrhenius dependence with $P_0 = 2.11 \times 10^{-15}$ $m^3 s^{-1}$ and $Q_{GB} = 81.24$ kJ mol^{-1}.

(3) Direct measurements of the GBD coefficient D_{GB} of Au in Cu were carried out in the C regime as well. The Arrhenius parameters $D_{GB}^0 = 4.87 \times 10^{-6}$ $m^2 s^{-1}$ and $H_{GB} = 91.03$ kJ mol^{-1} have been obtained.

(4) Combining the obtained P and D_{GB} values and taking $\delta = 0.5$ nm, the GB-segregation factor $s = P/D_{GB}\delta$ was determined. In the temperature interval 450–526 K the segregation factor decreases from 11 to 6 with an extrapolated value of about 2 at the melting point of Cu. From its temperature dependence, the segregation enthalpy $H_s = -9.7$ kJ mol^{-1} has been estimated. This value is

well consistent with previous experimental results for surface segregation in the Cu-Au system. Both GB and surface segregation in this system are most probably dominated by the atomic-size effect.

(5) Using the same experimental technique and the radiotracer ^{64}Cu, GB self-diffusion in Cu has been studied in the type-B regime at temperatures 784–973 K. The obtained Arrhenius parameters are $P_0 = 1.16 \times 10^{-15}$ m^3 s^{-1} and $Q_{GB} = 84.75$ kJ mol^{-1}.

(6) Although Au diffusion in the lattice of Cu is slightly faster than Cu self-diffusion, an opposite relation is observed for GBD. The effect is explained by trapping Au atoms to certain positions in the GB structure and formation of immobile complexes similar to 2D compounds.

(7) The GB diffusion and segregation characteristics of Au in Cu obtained in the present investigation are in good agreement with theoretical expectations for a system of homologous elements with complete solid solubility but with a difference in atomic radii. This agreement confirms that the outlined procedure of data evaluation in type-B and -C GBD regimes provides a tool to characterize average segregation and kinetic properties of general high-angle GB's from diffusion measurements on polycrystals.

ACKNOWLEDGMENTS

*Permanent address: Russian Institute of Aviation Materials, 107005 Moscow, Russia.

[1]K. Aoki and O. Izumi, Trans. Jpn. Inst. Met. 19, 203 (1978).

[2]I. Kaur and W. Gust, Fundamentals of Grain and Interphase Boundary Diffusion (Ziegler, Stuttgart, 1988).

[3]J. Bernardini and P. Gas, Defect Diffus. Forum 95-98, 393 (1993).

[4]J. Cabané and F. Cabané, Solid State Phenom. Diff. Defect Data 15-16, 1 (1991).

[5]P. Neuhaus and Chr. Herzig, Z. Metallkd. 80, 220 (1989).

[6]J. Bernardini, Defect Diffus. Forum 66-69, 667 (1989).

[7]J. C. Fisher, J. Appl. Phys. 22, 74 (1951).

[8]L. G. Harrison, Trans. Faraday Soc. 57, 1191 (1961).

[9]J. Bernardini, P. Gas, E. D. Hondros, and M. Seah, Proc. R. Soc. London Ser. A 378, 159 (1982).

[10]P. Gas, M. Guttman, and J. Bernardini, Acta Metall. 30, 1309 (1982).

[11]P. Gas, S. Poize, and J. Bernardini, Acta Metall. 34, 395 (1986).

[12]A. Atkinson and R. I. Taylor, Philos. Mag. A 43, 979 (1981).

[13]J. Sommer and Chr. Herzig, J. Appl. Phys. 72, 2758 (1992).

[14]Chr. Herzig, J. Geise, and Yu. Mishin, Acta Metall. Mater. 41, 1683 (1993).

[15]J. Geise, H. Mehrer, Chr. Herzig, and G. Weyer, in Vacancies and Interstitials in Metals and Alloys, Vols. 15–18 of Materials Science Forum, edited by C. Abromeit and H. Wollenberger (Trans Tech, Aedermannsdorf, 1987), p. 443.

[16]Binary Alloy Phase Diagrams, edited by T. B. Massalski (American Society for Metals, Metals Park, Ohio, 1986), Vol. 1, p. 75.

[17]W. Losch and J. Kirschner, J. Vac. Sci. Technol. 15, 1541 (1978).

[18]S. Fujikawa, M. Werner, H. Mehrer, and A. Seeger, in Vacancies and Interstitials in Metals and Alloys (Ref. 15), p. 431.

[19]K. Maier, Phys. Status Solidi B 44, 567 (1977).

[20]T. Suzuoka, Trans. Jpn. Inst. Met. 2, 25 (1961).

[21]A. E. Austin and N. A. Richard, J. Appl. Phys. 33, 3569 (1962).

[22]A. E. Austin, N. A. Richard, and V. E. Wood, J. Appl. Phys. 37, 3650 (1966).

[23]A. Chatterjee and D. J. Fabian, Acta Metall. 17, 1141 (1969).

[24]I. Kaur, W. Gust, and L. Kozma, Handbook of Grain and Interphase Boundary Diffusion Data (Ziegler, Stuttgart, 1989).

[25]A. N. Aleshin, B. S. Bokstein, V. K. Egorov, and P. V. Kurkin, Defect Diffus. Forum 95-98, 475 (1993).

[26]A. N. Aleshin, V. K. Egorov, B. S. Bokstein, and P. V. Kurkin, Thin Solid Films 223, 51 (1993).

[27]A. Vignes and J. P. Haeussler, Mem. Sci. Rev. Metall. 63, 1091 (1966).

[28]D. L. Johnson, J. Appl. Phys. 40, 192 (1969).

[29]B. Burton and G. W. Greenwood, Met. Sci. J. 4, 215 (1970).

[30]A. Hässner, Krist. Tech. 9, 1371 (1974).

[31]I. A. Szabo, D. L. Beke, and F. J. Kedves, Philos. Mag. A 62, 227 (1990).

[32]S. M. Klotsman, Defect Diffus. Forum 99-100, 25 (1993).

[33]V. N. Kaygorodov, S. M. Klotsman, A. N. Timofeyev, and I. S. Trakhtenberg, Phys. Met. Metallogr. 25, 910 (1968).

[34]J. M. McDavid and S. C. Fain, Surf. Sci. 52, 161 (1975).

[35]M. P. Seah, J. Phys. F 10, 1043 (1980).

[36]Selected Values of Thermodynamic Properties of Metals and Alloys, edited by R. Hultgren et al. (Wiley, New York, 1973).

[37]D. Gupta, in Diffusion Phenomena in Thin Films and Microelectronic Materials, edited by D. Gupta and P. S. Ho (Park Ridge, New York, 1988), p. 204.

[38]T. Muschik, W. Gust, S. Hofmann, and B. Predel, Acta Metall. 37, 2917 (1989).